Neuron, Volume *110*

Supplemental information

A sensitive GRAB sensor for detecting extracellular ATP *in vitro* and *in vivo*

Zhaofa Wu, Kaikai He, Yue Chen, Hongyu Li, Sunlei Pan, Bohan Li, Tingting Liu, Fengxue Xi, Fei Deng, Huan Wang, Jiulin Du, Miao Jing, and Yulong Li

Figure S1.

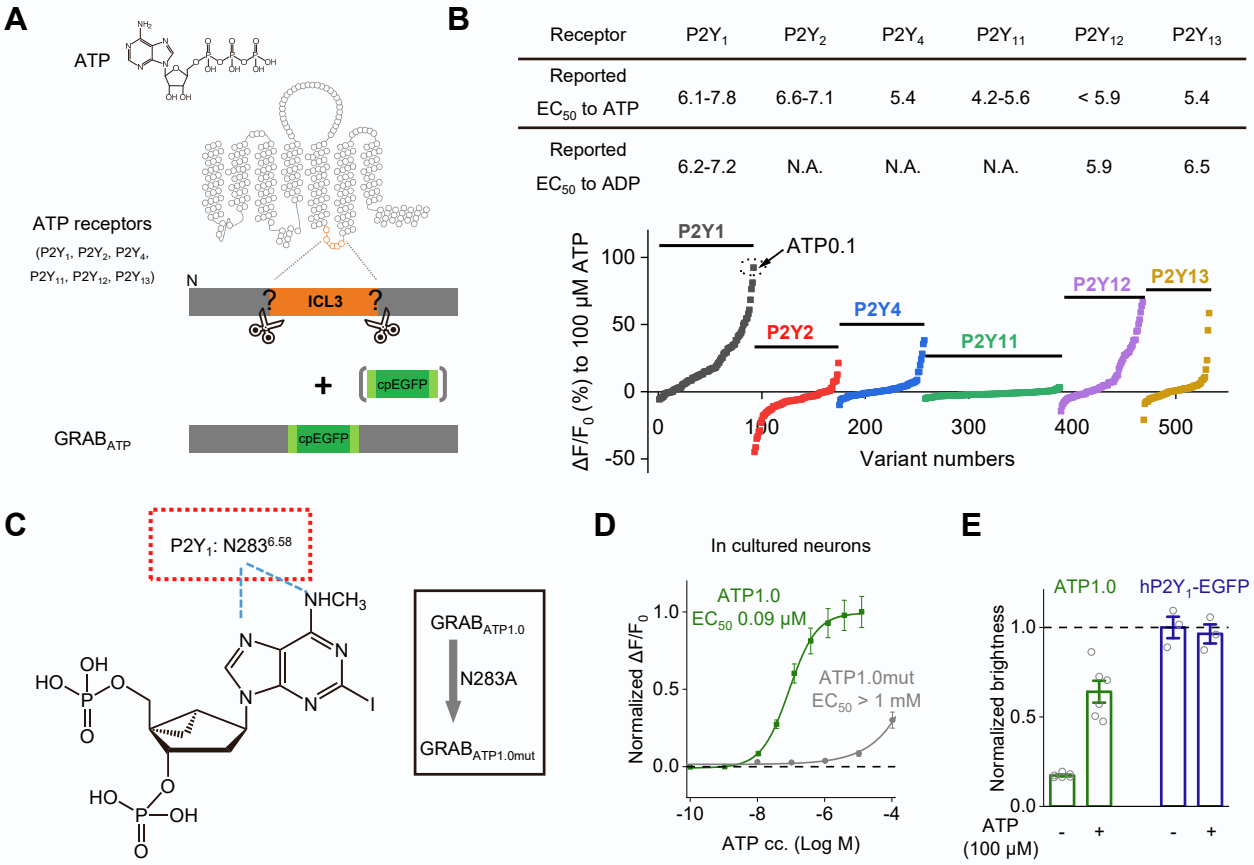

Receptor	$P2Y_1$	$P2Y_2$	$P2Y_4$	$P2Y_{11}$	$P2Y_{12}$	$P2Y_{13}$
Reported EC_{50} to ATP	6.1-7.8	6.6-7.1	5.4	4.2-5.6	< 5.9	5.4
Reported EC_{50} to ADP	6.2-7.2	N.A.	N.A.	N.A.	5.9	6.5

F

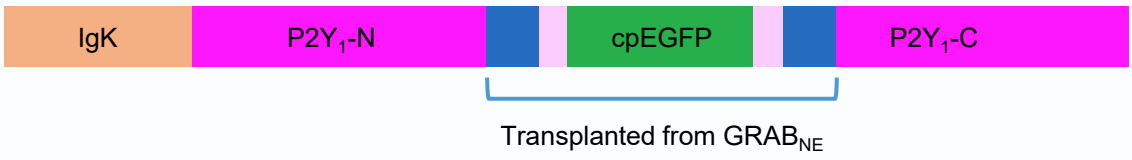


```
1   METDTLLLWVLLLWVPGSTGDTSLCEKVGTTEVLWPAVPNGTDAAFLAGP  50
51  GSSWGNSTVASTAAVSSSFKCALTKTGFQFYYLPAVYILVFIIGFLGNSV 100
101 AIWMFVFHMKPWSGISVYMFNLALADFLYVLTLPALIFYYFNKTDWIFGD 150
151 AMCKLQRFIFHVNLYGSILFLTCISAHRYSGVVYPLKSLGRLKKKNAICI 200
201 SVLVWLIVVVAISPILFYSGTGVRKNKTITCYDTTSDEYLRSYFIYSMCT 250
251 TVAMFCVPLVLILGCYGLIVRALIYPAPAGPRDTDALDLEEGGNVYIKAD 300
301 KQKNGIKANFHIRHNIEDGGVQLAYHYQQNTPIGDGPVLLPDNHYLSVQS 350
351 KLSKDPNEKRDHMVLLEFVTAAGITLGMDELYKGGTGGSMVRKGEELFTG 400
401 VVPILVELDGDVNGHKFSVSGEGEGDATEGKLTLKFICTTGKLPVPWPTL 450
451 VTTLTYGVQCFSRYPDHMKQHDFFKSAMPEGYIQERTIFFKDDGNYKTRA 500
501 EVKFEGDTLVNRIELKGIDFKEDGNILGHKLEYNTGAAARWRGRSIYLVI 550
                ATP1.0mut:
                N283A
551 IVLTVFAVSYIPFHVMKTMNLRARLDFQTPAMCAFNDRVYATYQVTRGLA 600
601 SLNSCVDPILYFLAGDTFRRRLSRATRKASRRSEANLQSKSEDMTLNILP 650
651 EFKQNGDTSL                                          700
```

Figure S1. Development and characterization of GRAB$_{ATP}$ sensors, related to Figure 1.

(A and B) Selection of a GPCR scaffold for designing a genetically engineered GRAB-based ATP sensor. **(A)** Schematic diagram depicting the strategy for screening candidate GPCR scaffolds. **(B)** Upper panel, summary of the reported EC_{50} values of six human P2Y GPCRs for ATP and ADP (https://www.guidetopharmacology.org/); bottom panel, selection of the cpEGFP insertion site in the six candidates based on the fluorescence response of each variant to 100 μM ATP. The final sensor, ATP1.0, is based on the hP2Y$_1$ receptor and is indicated. ICL3, third intracellular loop; GPCR, G protein–coupled receptor; N.A., not available.

(C and D) Design of an ATP-insensitive mutant sensor. **(C)** Location of N283, a key residue in the hP2Y$_1$ receptor for ligand binding; this residue in ATP1.0 was mutated to an alanine (N283A mutation), resulting in the ATP1.0mut sensor. **(D)** Normalized dose-dependent fluorescence changes in neurons expressing either ATP1.0 or ATP1.0mut in response to ATP, each point represents the average response measured in 12-14 ROIs.

(E) Summary of the normalized brightness of ATP1.0 and hP2Y$_1$-EGFP before (-) and after (+) 100 μM ATP application. Data collected from 3-6 wells.

(F) Full amino acid sequence of the ATP1.0 and ATP1.0mut sensors. The IgK leader sequence, cpEGFP moiety, and N-terminal and C-terminal portions of the hP2Y$_1$ receptor indicated.

Summary data are presented as the mean ± SEM.

Figure S2.

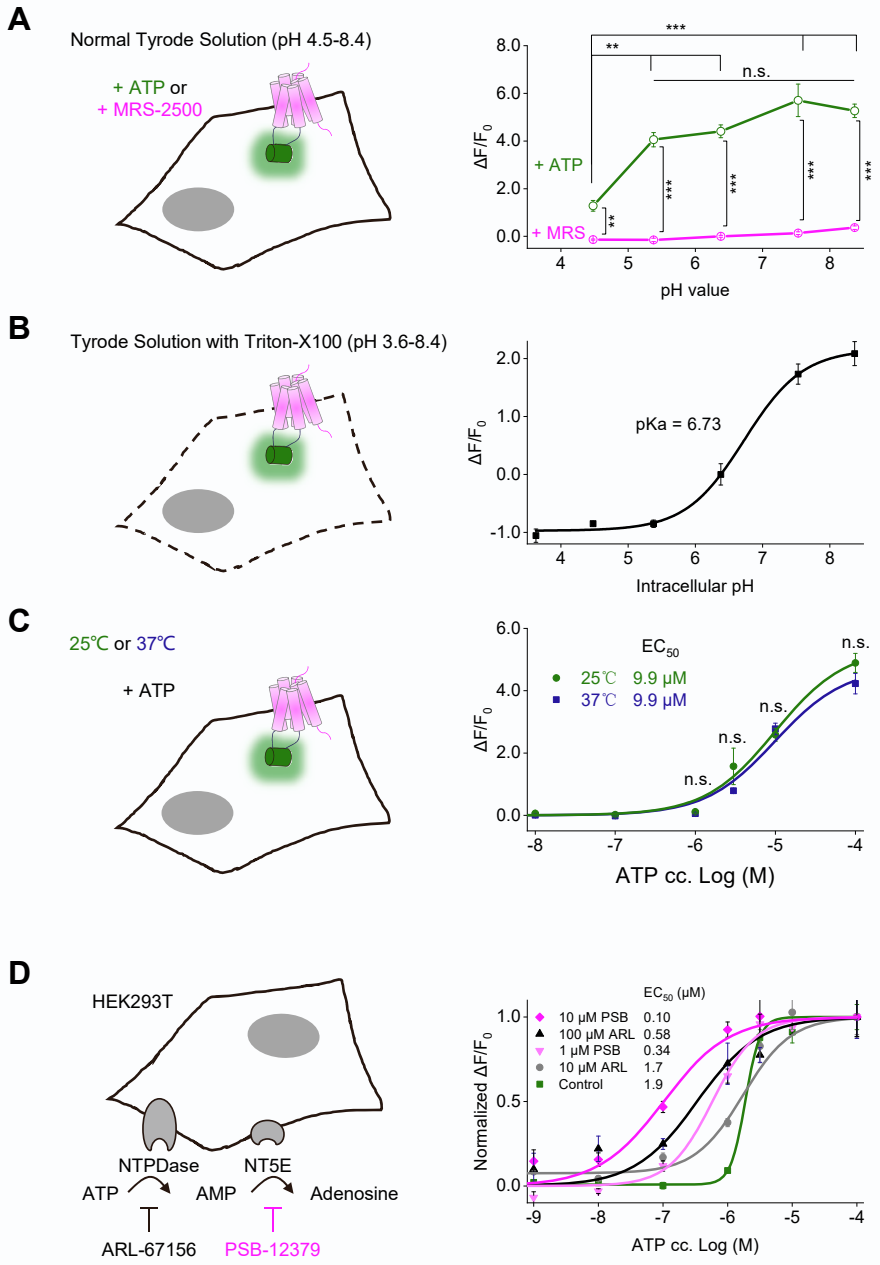
A
Normal Tyrode Solution (pH 4.5-8.4)
+ ATP or
+ MRS-2500
+ ATP
+ MRS
ΔF/F0
pH value
n.s.
B
Tyrode Solution with Triton-X100 (pH 3.6-8.4)
pKa = 6.73
Intracellular pH
C
25℃ or 37℃
+ ATP
EC50
25℃ 9.9 μM
37℃ 9.9 μM
n.s.
ATP cc. Log (M)
D
HEK293T
NTPDase
NT5E
ATP
AMP
Adenosine
ARL-67156
PSB-12379
EC50 (μM)
10 μM PSB 0.10
100 μM ARL 0.58
1 μM PSB 0.34
10 μM ARL 1.7
Control 1.9
Normalized ΔF/F0
ATP cc. Log (M)

Figure S2. The effect of pH, temperature and ectoATPase blockers on ATP1.0 signals, related to Figure 1.

(A) Left, schematic illustration of the experimental design used to measure the effects of bath applied ATP (green) and MRS-2500 (MRS, magenta) in ATP1.0-expressing HEK293T cells. Right, quantification for ATP and MRS-2500-induced fluorescence responses. Data collected from 3 wells (>100 ROIs per well).

(B) Left, schematic illustration of the experimental design used to measure the effects of bath applied buffers on fluorescence responses in ATP1.0-expressing HEK293T cells gently permeabilized by detergent Triton-X100 (0.3% for ~5 minutes). Right, quantification for the relative buffer-induced fluorescence responses. The fluorescence intensity of pH 6.4 was set as F_0 and the relative fluorescence changes in each pH value were plotted. Data collected from 3 wells (~2 x 10^5 cells per well).

(C) Left, schematic illustration of the experimental design used to measure the effects of temperature on fluorescence responses in ATP1.0-expressing HEK293T cells. Right, quantification for different concentrations of ATP induced fluorescence responses. Data collected from 4 wells (>100 ROIs per well).

(D) Left, schematic illustration of ARL-67156 (ARL) and PSB-12379 (PSB) that block NTPDase and NT5E, respectively. Right, dose-response curve for ATP1.0 sensors expressed in HEK293T cells in response to ATP when treated with different concentrations of ARL or PSB. Data were normalized to 100 μM ATP induced responses; data collected from 4 wells (>100 ROIs per well).

Summary data are presented as the mean ± SEM. The data shown in **(A)** were analyzed using a one-way ANOVA followed by Bonferroni's Multiple Comparison Test; the data shown in **(C)** were analyzed using Student's *t*-test; n.s. not significant.

Figure S3.

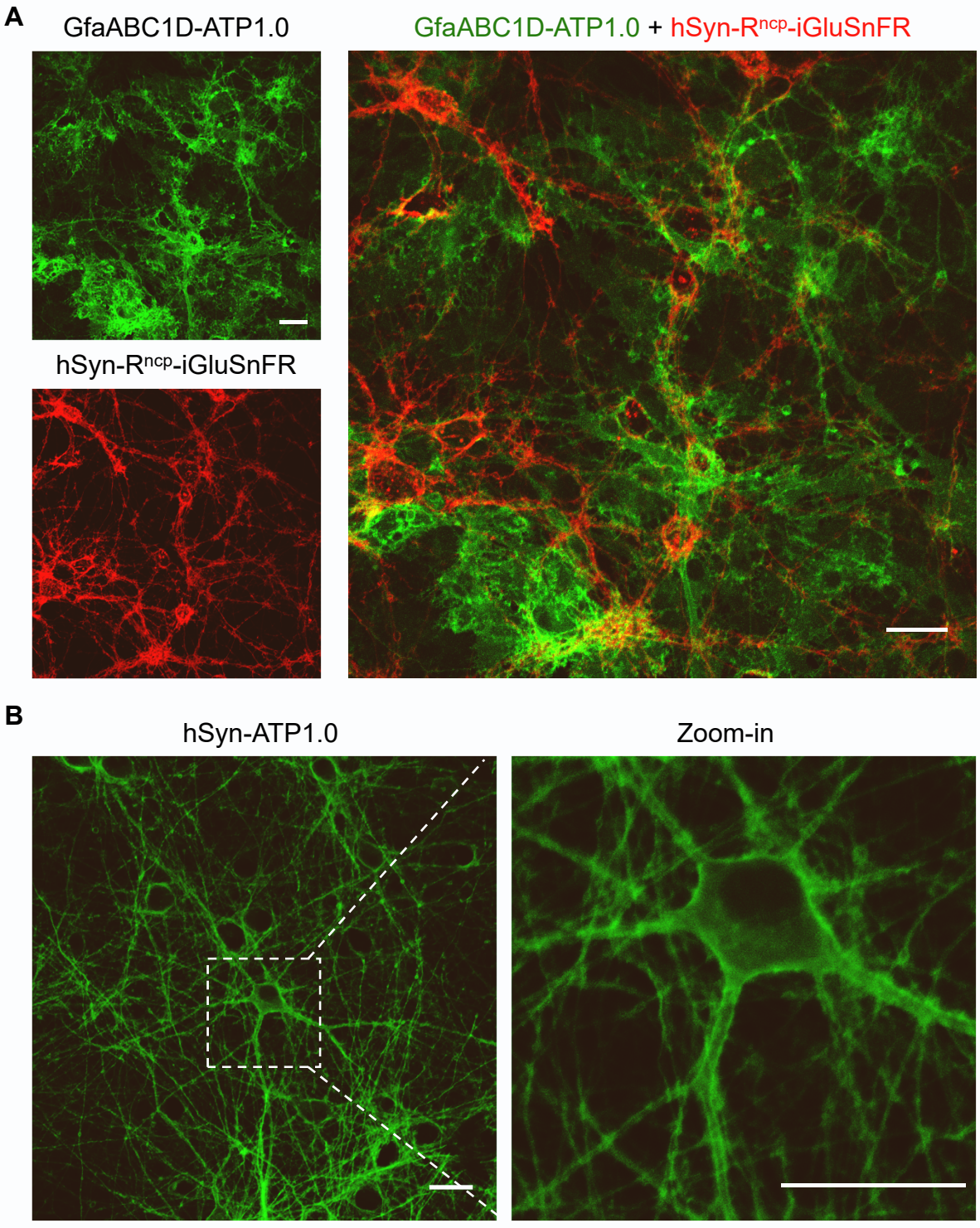

Figure S3. Expression of ATP1.0 in cultured neurons and astrocytes, related to Figure 2.

(A) Dual-color imaging of ATP1.0 expressed in astrocytes under the control of the astrocyte-specific GfABC1D promoter and R^{ncp}-iGluSnFR expressed in neurons under the control of the hSyn promoter.

(B) ATP1.0 was expressed in cultured rat cortical neurons under the control of the neuro-specific hSyn promoter.

Scale bars represent 30 μm.

Figure S4.

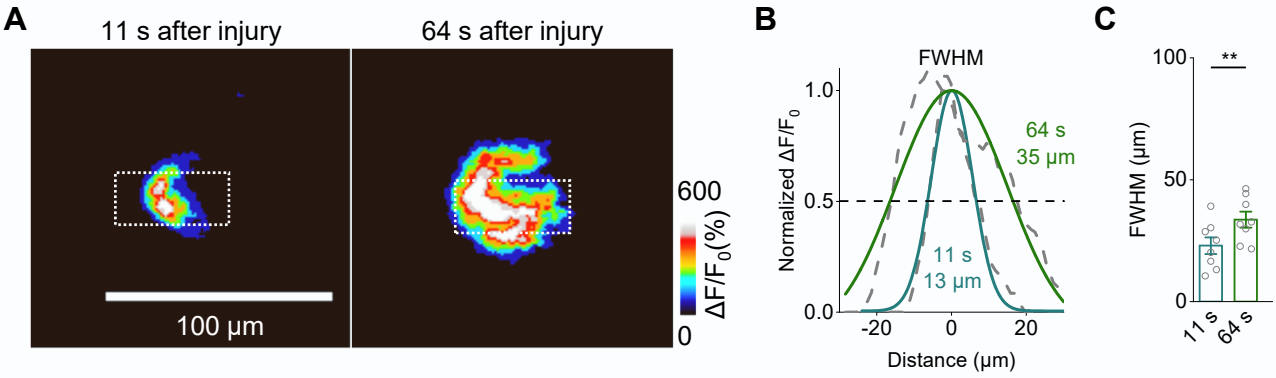

Figure S4. Spatial profile of the change in ATP1.0 fluorescence at different time after injury in a zebrafish model, related to Figure 4.

(A) Pseudocolor images showing the response of ATP1.0 at ~11 s and ~64 s after laser ablation in the optic tectum.

(B). Spatial profile of the change in ATP1.0 shown in **(A)**.

(C) Summary of the full width at half maximum FWHM.

Summary data are presented as the mean ± SEM, n = 6 fishes; Student's *t*-test, ***p*<0.01.

Figure S5.

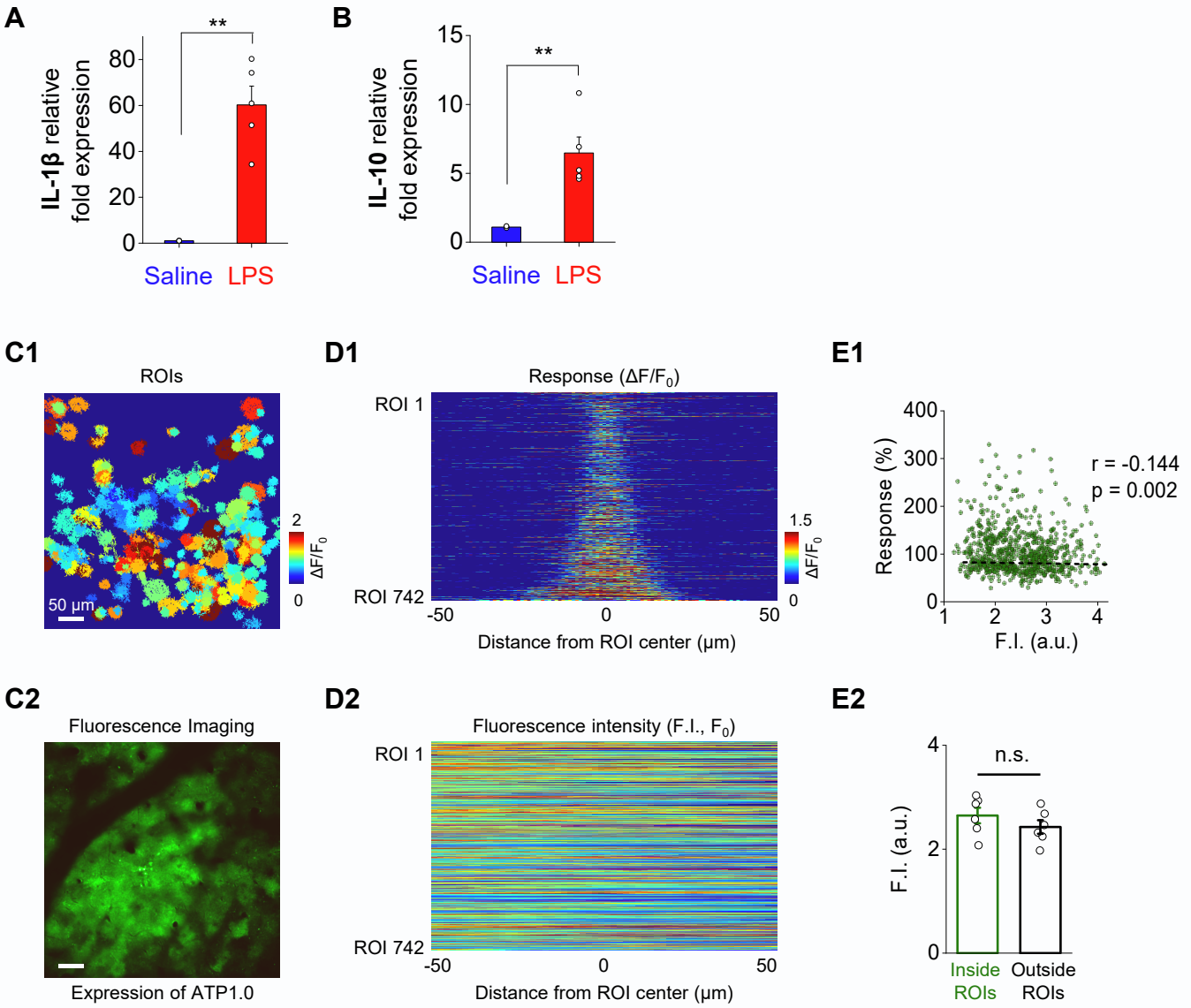

Figure S5. Imaging localized ATP-release events with ATP1.0 in the mouse brain following systemic inflammation induced by an injection of LPS, related Figure 5.

(A and B) Expression levels of IL-1β and IL-10 in the mouse brain 24 h after an intraperitoneal injection of saline or lipopolysaccharides (LPS). mRNA expression levels of the inflammatory cytokines IL-1β **(A)** and IL-10 **(B)** are measured in the brains of saline- and LPS-injected mice. GAPDH expression was used as an internal control for calculating the fold change in expression. n = 5 mice.

(C-E) Fluorescence responses and expression levels of ATP1.0 in living mice. **(C)** Images shown the fluorescence responses of region of interested (ROIs, **C1**) and expression of ATP1.0 **(C2)** after LPS injection. **(D)** The fluorescence response ($\Delta F/F_0$, **D1**) and the fluorescence intensity (F.I., F_0, **D2**) of different ROIs, n = 742 events from 6 mice. **(E1)** The relationship between fluorescent response and the fluorescent intensity; a.u., arbitrary unit. **(E2)** Quantification of the fluorescent intensity inside or outside of ROIs, n = 6 mice.

Summary data are presented as the mean ± SEM. Student's *t*-test; $^{**}p<0.01$; n.s., not significant.

Figure S6.

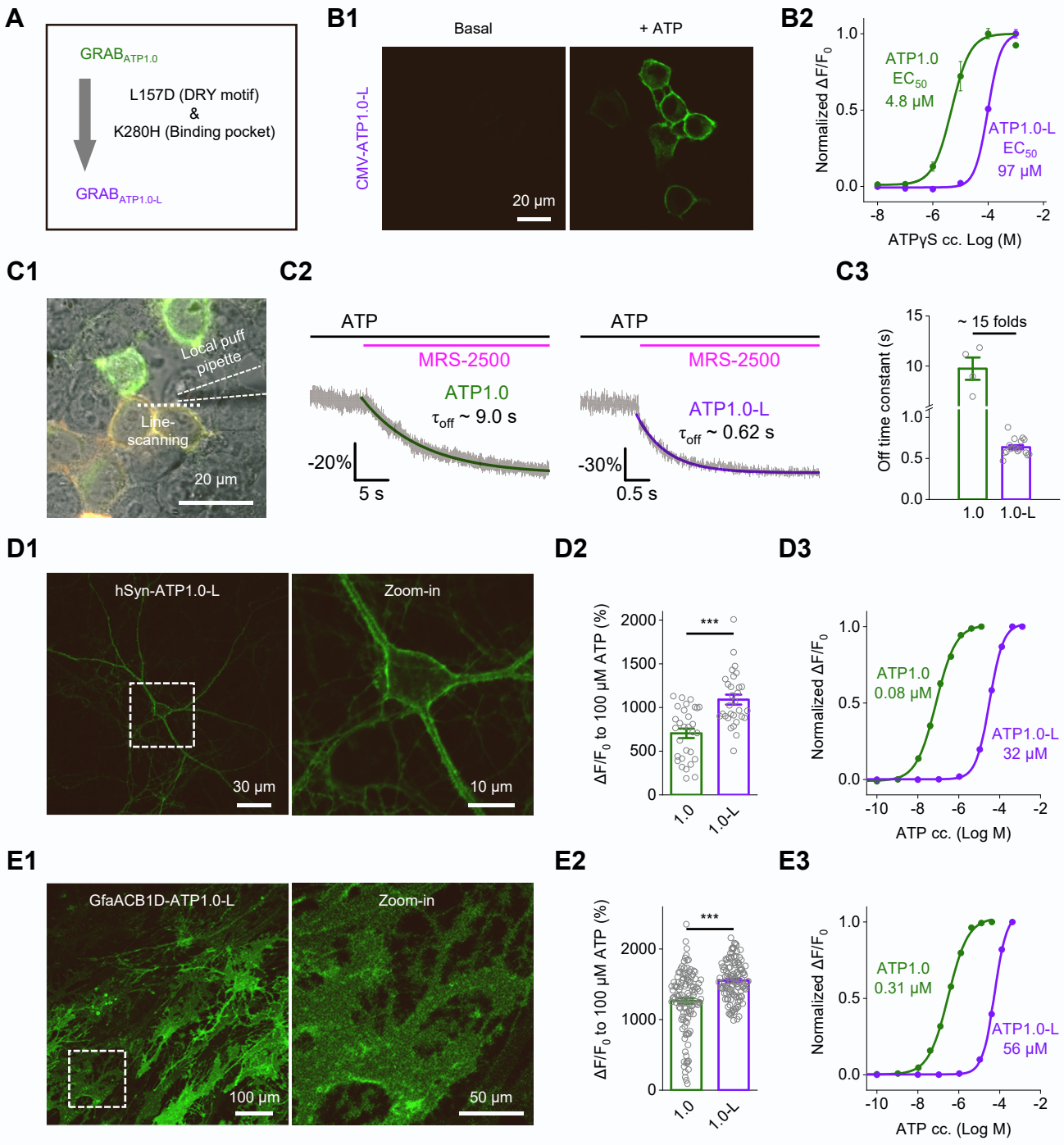
A
GRAB$_{ATP1.0}$
L157D (DRY motif)
&
K280H (Binding pocket)
GRAB$_{ATP1.0-L}$
B1
Basal
+ ATP
CMV-ATP1.0-L
20 μm
B2
Normalized ΔF/F$_0$
ATP1.0
EC$_{50}$
4.8 μM
ATP1.0-L
EC$_{50}$
97 μM
ATPγS cc. Log (M)
C1
Local puff pipette
Line-scanning
20 μm
C2
ATP
MRS-2500
ATP1.0
τ$_{off}$ ~ 9.0 s
-20%
5 s
ATP
MRS-2500
ATP1.0-L
τ$_{off}$ ~ 0.62 s
-30%
0.5 s
C3
~ 15 folds
Off time constant (s)
1.0
1.0-L
D1
hSyn-ATP1.0-L
30 μm
Zoom-in
10 μm
D2
ΔF/F$_0$ to 100 μM ATP (%)
***
1.0
1.0-L
D3
Normalized ΔF/F$_0$
ATP1.0
0.08 μM
ATP1.0-L
32 μM
ATP cc. (Log M)
E1
GfaACB1D-ATP1.0-L
100 μm
Zoom-in
50 μm
E2
ΔF/F$_0$ to 100 μM ATP (%)
***
1.0
1.0-L
E3
Normalized ΔF/F$_0$
ATP1.0
0.31 μM
ATP1.0-L
56 μM
ATP cc. (Log M)

Figure S6. Development and characterization of a low affinity ATP sensor, ATP1.0-L, in cultured cells, related to Figure 1 and Figure 2.

(A) Introducing L157D and K280H mutations of in ATP1.0, resulting in the $GRAB_{ATP1.0\text{-}L}$ (ATP1.0-L) sensor.

(B) Expression and affinity of ATP1.0-L in HEK293T cells. **(B1)** Example fluorescence images of HEK293T cells expressing the ATP1.0-L sensor under basal conditions and in the presence of 100 μM ATP. **(B2)** Normalized dose-response curves of ATP1.0 (green) and ATP1.0-L (violet) in response to ATPγS, n = 3 wells each with >100 ROIs per well.

(C) The response kinetics of ATP1.0 and ATP1.0-L. **(C1)** Schematic illustration showing the local perfusion system. **(C2)** Representative traces showing the response of ATP1.0 (Left) and ATP1.0-L (Right) to ATP and subsequent addition of MRS-2500. Each trace was fitted with a single-exponential function to determine τ_{off}. **(C3)** Group summary of τ_{off} of ATP1.0 and ATP1.0-L. n = 4 from 4 coverslips for ATP1.0 and n = 17 from 8 coverslips for ATP1.0-L.

(D and E) Characterization of ATP1.0-L in rat cortical neuron-glia co-cultures. **(D)** ATP1.0-L was expressed in cultured neurons under control of hSyn promoter. **(D1)** Representative fluorescence images of neurons expressing the ATP1.0-L sensor in the presence of ATP. **(D2)** Summary of the $\Delta F/F_0$ after application of 100 μM ATP; n = 30 ROIs each from 3 coverslips. **(D3)** Normalized dose-response curves of ATP1.0 (green) and ATP1.0-L (violet) in response to ATP; n = 36-120 ROIs from 3 coverslips each; data for ATP1.0 was replotted from Figure 2I. **(E)** Same as **(D)**, except ATP1.0-L was expressed in cultured astrocytes under control of GfaACB1D promoter; n = 120 ROIs each from 3 coverslips.

Summary data are presented as the mean ± SEM. Student's *t*-test; ***$p<0.001$.

Figure S7.

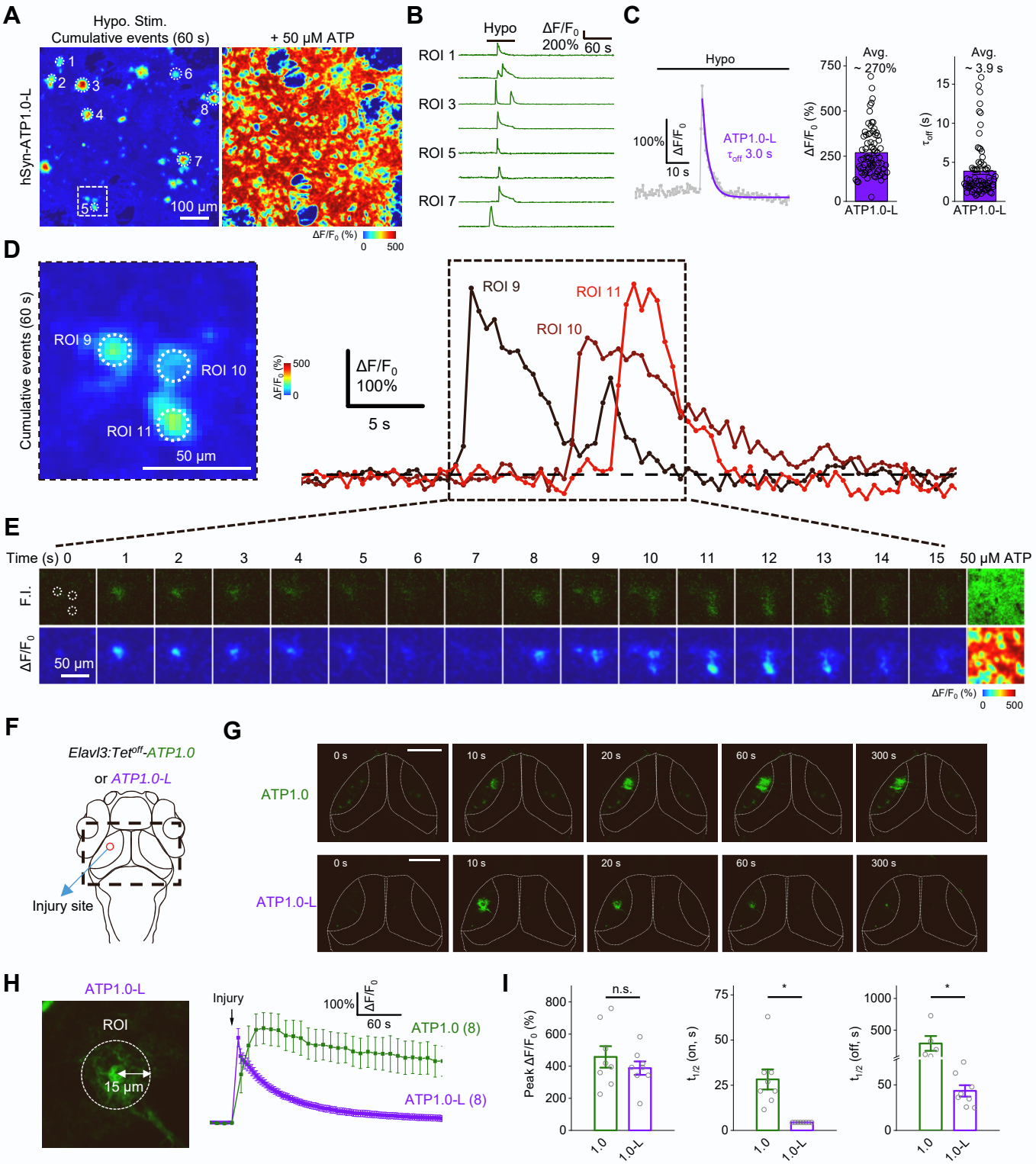
A
Hypo. Stim.
Cumulative events (60 s)
+ 50 μM ATP
hSyn-ATP1.0-L
100 μm
ΔF/F0 (%)
0
500
B
Hypo
ΔF/F0
200%
60 s
ROI 1
ROI 3
ROI 5
ROI 7
C
Hypo
100%
ΔF/F0
10 s
ATP1.0-L
τoff 3.0 s
Avg.
~ 270%
ΔF/F0 (%)
ATP1.0-L
Avg.
~ 3.9 s
τoff (s)
ATP1.0-L
D
Cumulative events (60 s)
ROI 9
ROI 10
ROI 11
50 μm
ΔF/F0 (%)
ΔF/F0
100%
5 s
E
Time (s)
50 μM ATP
F.I.
ΔF/F0
50 μm
F
Elavl3:Tetoff-ATP1.0
or ATP1.0-L
Injury site
G
ATP1.0
ATP1.0-L
0 s
10 s
20 s
60 s
300 s
H
ATP1.0-L
ROI
15 μm
Injury
100%
ΔF/F0
60 s
ATP1.0 (8)
ATP1.0-L (8)
I
Peak ΔF/F0 (%)
n.s.
t1/2 (on, s)
*
t1/2 (off, s)
*
1.0
1.0-L

Figure S7. ATP1.0-L can be used to detect ATP release in cultured neurons and in living zebrafish larvae, related to Figure 3 and Figure 4.

(A-E) Detecting localized ATP release with ATP1.0-L in cultured neurons. **(A)** Cumulative changes in ATP1.0-L fluorescence measured during 60 s of hypotonic stimulation (Hypo. Stim.) and ATP application. The white dashed circles indicate the regions of interest (ROI) used for analysis in **(B and C)**; the white dashed rectangles indicate the ROIs used for analysis in **(D and E)**. **(B and C)** Exemplar traces and temporal profile of the fluorescence response ($\Delta F/F_0$) of ATP1.0-L; n = 71-73 ROIs from 5 cultures. **(D)** Enlarged images and traces of 3 individual ROIs. **(E)** Time-lapse raw fluorescent images (upper) and response images (bottom).

(F-I) Imaging ATP release with ATP1.0-L in living zebrafish larvae. **(F)** Schematic diagram depicting imaging of ATP1.0 responses before and after laser ablation in the optic tectum of zebrafish larvae expressing ATP1.0 or ATP1.0-L. The red dashed circle indicates the region of laser ablation, and the black dashed rectangle indicates the imaging region shown in **(G)**. Scale bars represent 100 μm. **(G)** Time-lapse fluorescent images of ATP1.0 and ATP1.0-L to laser ablation in the optic tectum. The laser ablation was performed at time 0 s and lasted for approximate 7-sec. **(H)** Left, the white dashed circle indicates the region of interest (ROI, 15 μm in radius with the injury site as the center). Right, time course of the ATP1.0 (green) and ATP1.0-L (violet) response, the arrow indicates the beginning of the laser ablation, the numbers in parentheses represent the number of zebrafish larvae in each group. **(I)** Group summary of the peak $\Delta F/F_0$ in response (left), on ($t_{1/2}$, middle) and off ($t_{1/2}$, right) kinetics to laser ablation. n = 5-8 fish; Student's *t*-test; **p*<0.05; n.s., not significant (*p*>0.05).

Summary data are presented as the mean ± SEM.